JOURNAL OF SOLID STATE CHEMISTRY **124,** 381–384 (1996)
ARTICLE NO. 0253

BRIEF COMMUNICATION

The Room Temperature Crystal Structure of the Perovskite $Pr_{0.5}Sr_{0.5}MnO_3$

D. N. Argyriou,* D. G. Hinks, J. F. Mitchell, C. D. Potter, A. J. Schultz,†
D. M. Young,† J. D. Jorgensen, and S. D. Bader

*Material Science Division, *Science and Technology Center for Superconductivity, and †Intense Pulsed Neutron Source, Argonne National Laboratory, Argonne, Illinois 60439*

Received March 20, 1996; accepted April 22, 1996

Using both powder and single crystal neutron diffraction we have determined the room temperature structure of $Pr_{0.5}Sr_{0.5}MnO_3$ from melt-grown crystalline material. Contrary to previous measurements on polycrystalline samples we find the room temperature structure of $Pr_{0.5}Sr_{0.5}MnO_3$ is tetragonal, space group $F4/mmc$ ($a = 7.64093(5)$ Å, $c = 7.79104(8)$ Å). The structure of $Pr_{0.5}Sr_{0.5}MnO_3$ is related to the ideal primitive cubic perovskite structure by a single correlated rotation of MnO_6 octahedra about the c axis. We find that MnO_6 octahedra exhibit a small Jahn–Teller distortion (Δ(Mn–O) $\approx$ 0.02 Å).

Recent magnetic and transport measurements of manganite perovskites with composition $R_{0.5}Sr_{0.5}MnO_3$ (R = Pr, Nd) have shown a first-order transition from a ferromagnetic metal (FM) to an antiferromagnetic insulator (AFI) at ~150 K (1, 2). The FM state in manganite perovskites is attributed to the double exchange mechanism (3); localized t_{2g} spins are ferromagnetically coupled to itinerant e_g electrons. An interesting feature of these materials is that in the antiferromagnetic regime a charge ordered lattice of Mn^{3+} and Mn^{4+} ions is formed (4). Application of a magnetic field below 140 K has been shown to suppress the AFI state and presumably collapse the charge ordered lattice in favor of the FM state (2, 4). Previous structural studies on a polycrystalline sample of $Pr_{0.5}Sr_{0.5}MnO_3$ have shown that this material crystallizes wtih orthorhombic symmetry (*Pbnm*) (5). However, transport data on the same polycrystalline sample do not show a metal to nonmetal transition as reported by Tomioka *et al.* (2) and Kuwahara *et al.* (1) for single crystal specimens. In this communication we report the results of a detailed structural investigation at room temperature of a crystalline specimen of $Pr_{0.5}Sr_{0.5}MnO_3$ grown by the floating zone technique. We find that the room temperature structure is not orthorhombic, as previously reported, but tetragonal ($F4/mmc$), with a small Jahn–Teller (JT) distortion of the MnO_6 octahedral network.

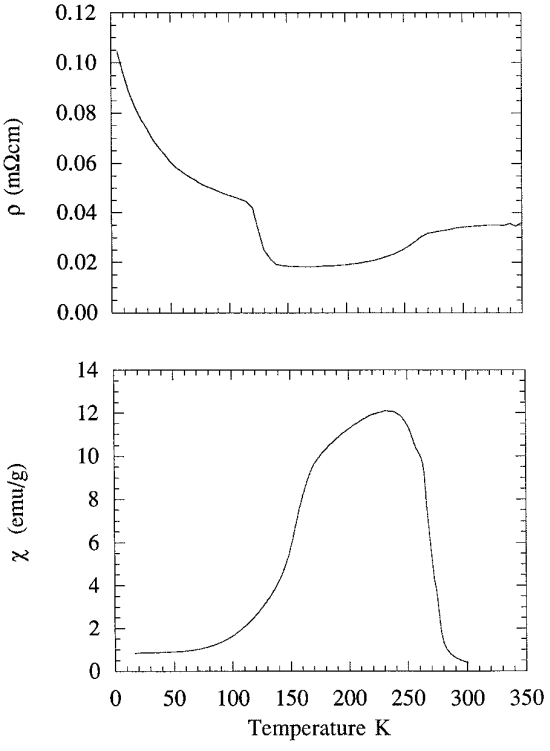

FIG. 1. Resistivity (upper panel) and ac susceptibility (lower panel) of $Pr_{0.5}Sr_{0.5}MnO_3$. Resistivity was measured in zero field while ac susceptibility was measured in a field of 10 Oe and a frequency of 100 Hz.

Crystals of $Pr_{0.5}Sr_{0.5}MnO_3$ were melt-grown in oxygen at 2 bars using a floating zone arc image furnace (NEC SC-M15HD) equipped with double hemiellipsoidal mirrors. The growth rate on the feed and seed rods was 2.5

0022-4596/96 $18.00

TABLE 1
Crystal Data and Experimental Parameters

Chemical formula	$Pr_{0.5}Sr_{0.5}MnO_3$
Crystal system	Tetragonal
Space group	*F*4/*mmc*
a (Å)	7.64093(5)
c (Å)	7.79104(8)
Z	8
d-spacing range	0.5–4 Å
No. of points in pattern	5152
No. of reflections	282
Number of refined parameters	28
R_{wp}(%)	5.67
$R(F^2)$	6.02
R_{exp}/R_{obs}	1.4

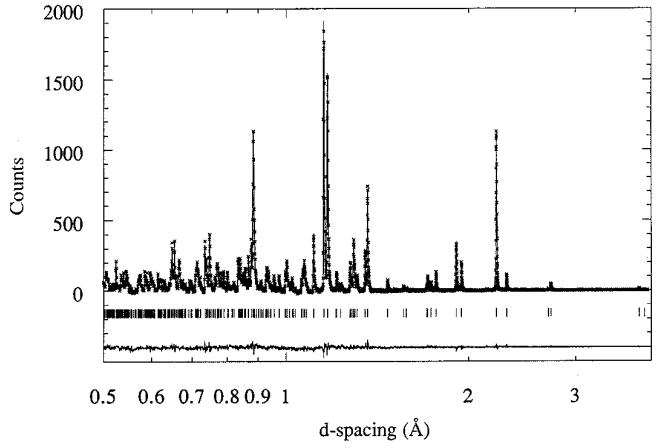

FIG. 2. Observed (crosses) and calculated (solid line) diffraction patterns of $Pr_{0.5}Sr_{0.5}MnO_3$ measured at room temperature. The location of expected reflections and the difference between observed and calculated patterns are shown beneath. The background has been subtracted. The *x* axis is plotted on a logarithmic scale to illustrate better the fit to the data at smaller *d* spacings.

and 2.0 mm/h, respectively. The feed and seed rods were rotated in opposite directions at 35 and 30 rpm, respectively. After growth, the boule was annealed in flowing oxygen at 1200°C for 24 h. The sample was characterized using both four-probe resistivity (Quantum design PPMS) and ac susceptibility (Lake Shore Cryotronics Model 7000 ac susceptometer). Figure 1 shows the temperature dependence of both the resistivity (upper) and ac magnetic susceptibility (lower). Both are in agreement with the measurements of Tomioka *et al.* (2) on single crystal specimens. As is evident from these measurements the sample is a paramagnetic conductor at room temperature.

Pieces from the same boule were studied using both neutron powder diffraction (from pulverized crystals) and single crystal time-of-flight neutron diffraction. Powder patterns were measured using the Special Environment Powder Diffractometer (SEPD) (6) while single crystal data were measured using the Single Crystal Diffractometer (SCD) (7) both operating at Argonne's Intense Pulsed Neutron Source. Diffraction data were collected at room temperature. Rietveld analysis of the powder data was carried out using the program GSAS (8). In the analysis, background, peak width, absorption, and extinction parameters were refined, together with lattice parameters, an atomic position for one oxygen atom (see Table 2), fractional occupancies for the *A*- and *B*-site cations, and anisotropic temperature factors for both cations and oxygen. Experimental details and crystal data are given in Table 1.

Integrated Bragg intensities were measured from a crystal sample using SCD, covering one octant of reciprocal space, over the nominal *d*-spacing range from 0.5 to 3 Å. Observed reflections were best indexed using a face centered tetragonal cell, with dimensions $2a \times 2a \times 2a$, where *a* is the primitive cubic perovskite lattice parameter. Full refinement of the SCD data was prohibited due to twinning of the crystal thus the structure was determined using only the powder data. Rietveld refinement of the powder data was performed using space group *F*4/*mmc* (No. 140, a setting of *I*4/*mcm*), a space group predicted by Glazier (9) for perovskite-type materials with the observed $2a \times 2a \times 2a$ cell dimensions. This model produced an excellent fit to the observed powder data (Fig. 2). Rietveld analysis of the powder data using the previously reported orthorhombic structure (5) failed to converge and resulted in very poor fits. Refined occupancies and structural and thermal parameters are given in Table 2.

The room temperature structure of $Pr_{0.5}Sr_{0.5}MnO_3$ is

TABLE 2
Atomic Parameters, Fractional Occupancies, and Anisotropic Temperature Factors for $Pr_{0.5}Sr_{0.5}MnO_3$

Atom	*x*	*y*	*z*	Occup.	$100 \times U_{11}$	$100 \times U_{22}$	$100 \times U_{33}$
Pr/Sr	1/4	1/4	1/4	0.94(1)	0.57(4)	0.57(4)	0.74(6)
Mn	0	0	0	1.00(1)	0.79(5)	0.79(5)	0.42(7)
O1	0	0	1/4	1.0	1.90(4)	1.90(4)	0.95(6)
O2	1/4	0.0337(1)	0	1.0	0.92(4)	1.49(4)	1.79(5)

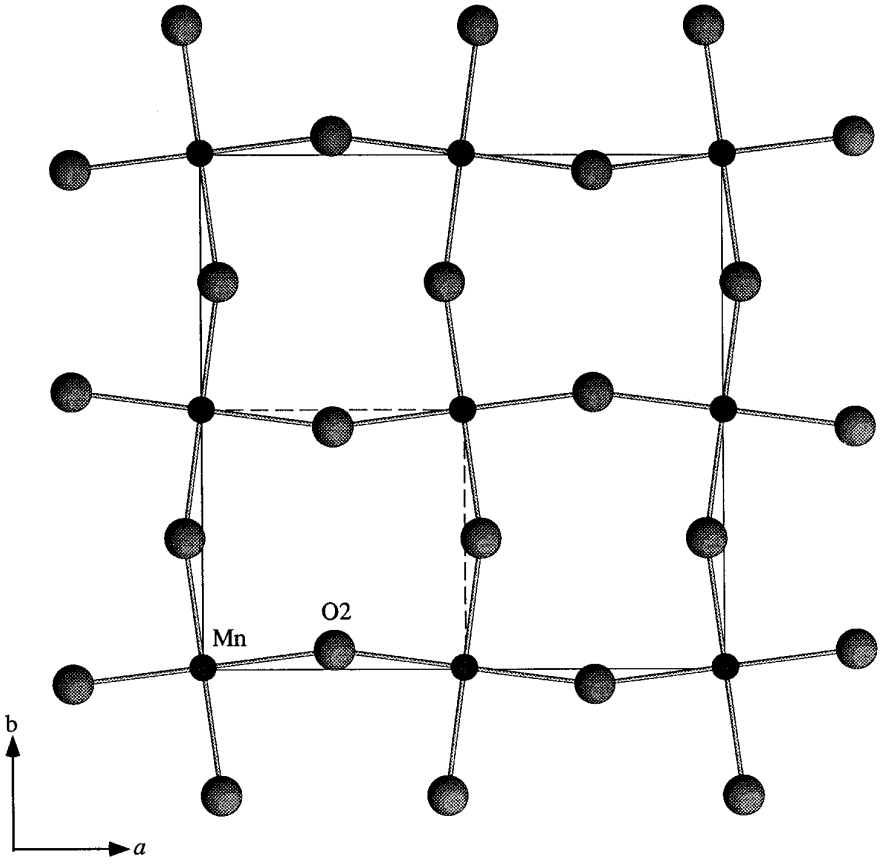

FIG. 3. Projections onto the (001) plane of the $Pr_{0.5}Sr_{0.5}MnO_3$ structure at room temperature. The solid line represents the observed tetragonal cell while the broken line represents the primitive cubic perovskite cell.

related to the ideal primitive cubic perovskite structure by a single correlated rotation of MnO_6 octahedra about the *c*-axis, as illustrated in Fig. 3. The rotation of MnO_6 octahedra is of the same magnitude but opposite in sign between adjacent layers along the *c* axis. This rotation results in a tilt between MnO_6 octahedra along the *a* or *b* axis, producing a Mn–O–Mn bond angle of 164.64(5)°; there is not tilt present along the *c* axis. In Glazier's (9) notation this is a $a^0a^0c^-$ tilt system. This structure results in two different Mn–O distances; the first is between Mn and the equatorial oxygens that lie in the *a*–*b* plane (Mn–O2), while the second is with axial oxygens along the *c* axis (Mn–O1).

TABLE 3
Selected Bond Distances (Å) and Angles (°) for $Pr_{0.5}Sr_{0.5}MnO_3$

Mn–O1 (×2)	1.94776(2)	Mn–O1–Mn	180
Mn–O2 (×4)	1.9275(1)	Mn–O2–Mn	164.64(5)
Pr/Sr–O1 (×4)	2.70148(2)		
Pr/Sr–O2 (×4)	2.5546(5)		
(×4)	2.9143(6)		

Selected bond lengths and angles are given in Table 3. The MnO_6 octahedra exhibit a small Jahn–Teller (J-T) distortion (four short and two long Mn–O bonds), with the difference between axial and equatorial Mn–O distances being ~0.02 Å. The small distortion of MnO_6 octahedra is consistent with both the high concentration of Mn^{4+} (nominally 50%), a JT inactive ion, and the room temperature resistivity, which indicates delocalized e_g electrons.

Refinement of the occupancies of the cation sites showed that the Mn site was fully occupied, while the *A* site was deficient (occupancy = 0.94(1)), on the basis of the nominal Pr/Sr ratio. Another possible interpretation of this result involves a deviation from the nominal composition. If we assume full *A*-site occupancy, the Pr/Sr ratio obtained from Rietveld refinement is 0.63/0.37, substantially different from the nominal composition of 0.5 : 0.5. On the basis of a Rietveld refinement alone we cannot distinguish between these two possibilities.

We have determined the room temperature structure of $Pr_{0.5}Sr_{0.5}MnO_3$ from a melt grown crystalline sample. Contrary to previous studies on polycrystalline samples, we find that the room temperature structure of this material is tetragonal (*F*4/*mmc*) with the cell doubled along the *a*,

b, and *c* axis with respect to the primitive perovskite cell. In this metallic regime, MnO_6 octahedra show a small JT distortion. We have also measured the temperature dependence of the crystal structure from this sample to 20 K, the results of which will be published elsewhere.

ACKNOWLEDGMENTS

This work was supported by the NSF Office of Science and Technology Centers under (DMR 91-20000) (DNA), by an appointment to the U.S. Department of Energy Distinguished Postdoctoral Research Program sponsored by the U.S. Department of energy, Office of Science Education and Technical Information, and administered by the Oak Ridge National Laboratory (JFM), and by the U.S. Department of Energy, Basic Energy Sciences-Materials Sciences, and ER-LTT, under Contract W-31-109-ENG-38 (CDP,DGH,JDJ,SDB)

REFERENCES

1. H. Kuwahara, Y. Tomioka, A. Asamitsu, and Y. Tokura, *Science* **270,** 961 (1995).
2. Y. Tomioka, A. Asamitsu, Y. Moritomo, H. Kuwahara, and Y. Tokura, *Phys. Rev. Lett.* **74,** 5108 (1995).
3. C. Zener, *Phys. Rev.* **51,** 403 (1951).
4. E. O. Wollan and W. C. Koehler, *Phys. Rev.* **100,** 545 (1955).
5. K. Knízek, Z. Jirák, E. Pollert, and F. Zounová, *J. Solid State. Chem.* **100,** 292 (1992).
6. J. D. Jorgensen, J. J. Faber, J. M. Carpenter, R. K. Crawford, J. R. Haumann, R. L. Hitterman, R. Kleb, G. E. Ostrowski, F. J. Rotella, and T. G. Worton, *J. Appl. Crystallogr.* **22,** 321 (1989).
7. A. J. Schultz, *Trans. Am. Crystallogr. Assoc.* **23,** 61 (1987).
8. A. C. Larson and R. B. von Dreele, ''General Structure Analysis System'' University of California, Berkeley, 1985–1990.
9. A. M. Glazer, *Acta Crystallogr. A* **31,** 756 (1975).